LncRNA GAS5 attenuates fibroblast activation through inhibiting Smad3-mediated myofibroblast marker gene expression.

Rui Tang[2+#], Yung-Chun Wang[1+], Xiaohan Mei[1,2+], Ning Shi[1], Chengming Sun[2], Ran Ran[2], Gui Zhang[2], Wenjing Li[2], and Kevin Staveley-O'Carroll[1], Guangfu Li[1], Shi-You Chen[1,2*]

[1]Department of Surgery, University of Missouri School of Medicine, Columbia, MO 65212;
[2]Department of Physiology & Pharmacology, University of Georgia, Athens, GA, 30602;
[3]Department of Medical Pharmacology & Physiology, University of Missouri, Columbia, MO 65212

Running title: GAS5 in fibroblast activation.

[+]These authors contribute equally to this paper
[#]Current address: Department of Genetics, Stanford University School of Medicine, Stanford, CA 94305

*To whom correspondence should be addressed: Department of Surgery, University of Missouri School of Medicine, 1 Hospital Drive, Columbia, MO 65212, Tel: (573) 884-0371; Fax: (573) 884-4585; Email: scqvd@missouri.edu

Keywords: LncRNA, GAS5, TGF-β, fibroblast activation, skin fibrosis

Abstract:

Transforming Growth Factor β (TGF-β)-induced fibroblast activation is a key pathological event during tissue fibrosis. Long noncoding RNA (LncRNA) is a class of versatile gene regulators participating in various cellular and molecular processes. However, the function of lncRNA in fibroblast activation is still poorly understood. In this study, we identified growth arrest-specific transcript 5 (GAS5) as a novel regulator for TGF-β-induced fibroblast activation. GAS5 expression was downregulated in cultured fibroblasts by TGF-β and in resident fibroblasts isolated from bleomycin-treated skin tissues. Overexpression of GAS5 suppressed TGF-β-induced fibroblast to myofibroblast differentiation. Mechanistically, GAS5 directly bound Smad3 and promoted Smad3 binding to PPM1A, a Smad3 dephosphatase, and thus accelerated Smad3 dephosphorylation in TGF-b-treated fibroblasts. GAS5 also inhibited fibroblast proliferation. Importantly, local delivery of GAS5 via adenoviral vector suppressed bleomycin-induced skin fibrosis in mice. Collectively, our data revealed that GAS5 suppresses fibroblast activation and fibrogenesis through inhibiting TGF-β/Smad3 signaling, which provides a rationale for developing a LncRNA-based therapy to treat fibrotic diseases.

Introduction

Fibroblast activation is one of the important processes responsible for organ/tissue fibrosis, which is a wound healing progress following tissue/organ injury. The normal parenchymal tissue is gradually replaced by connective tissue accompanied by deposition of extraocular matrix (ECM) components during the fibrogenesis [1-3]. The pathogenesis of fibrosis is initiated in the residential area. The injury triggers innate immune response and causes recruitment of immune cells to the local area [4-6]. Pro-fibrotic cytokines or growth factors such as transforming growth factor β (TGF-β) secreted from circulating monocytes and residential macrophages induce fibroblast activation through fibroblast-myofibroblast transition [7-10]. Activated fibroblasts proliferate and thus increases tissue mass. In the meanwhile, myofibroblasts express extracellular matrix proteins such as collagen 1A (Col1A), the main component of excessive ECM deposition in human fibrotic diseases such as skin, cardiovascular, pulmonary, and liver cirrhosis. [11, 12].

TGF-β signaling regulates a wide spectrum of cellular processes, including cell differentiation, proliferation, migration, and apoptosis [13, 14]. TGF-β induces fibrosis through inducing fibroblast differentiation into collagen-producing myofibroblasts and increasing fibroblast proliferation [15, 16]. TGF-β transduces its signal mainly through Smad-dependent pathways. TGF-β binds and activates TGF-β receptors (TβRs), leading to Smad phosphorylation and translocation into nuclei where it activates the transcription of target genes [17, 18]. However, how Smad signaling is modulated is not completely understood.

Long non-coding RNAs (lncRNAs) are non-coding RNA molecules longer than 200 nucleotides. LncRNA is a class of versatile regulators which regulate gene expression at various levels ranging from chromatin modulation to protein degradation [19-21]. Growth Arrest Specific 5 (GAS5) is a well-known lncRNA that suppresses cell proliferation and induces apoptosis [22, 23]. Our previous studies have identified GAS5 as a regulator in both Smad3-dependent cell differentiation and p53-dependent cell survival [24, 25]. Since TGF-β signaling regulates both Smad-dependent fibroblast-myofibroblast transition and fibroblast proliferation during fibrosis, we hypothesized that GAS5 may be involved in TGF-β-induced fibroblast activation and fibrosis.

In the current study, we firstly found that GAS5 was downregulated in TGF-β-treated fibroblast cells and bleomycin-injected skin tissues. By both gain-of- and loss-of-function studies, we discovered that GAS5 suppressed TGF-β-induced fibroblast-myofibroblast transition through modulating Smad3 signaling/function. Mechanistically, GAS5 directly bound to Smad3, which enhanced phosphatase PPM1A binding to Smad3, and thus accelerated Smad3 dephosphorylation. GAS5 also inhibited fibroblast proliferation by blocking c-Jun N-terminal kinase (JNK) signaling pathway. In vivo, local delivery of adenoviral vector expressing GAS5 inhibited bleomycin-induced skin fibrosis in mice.

Results

GAS5 expression was decreased in TGF-β-activated fibroblasts.

TGF-β activated fibroblasts as shown by the induction of myofibroblast marker αSMA and Col1A in both 3T3 fibroblasts and primary cultured mouse skin fibroblasts (Fig. 1A-1D). To test if GAS5 is involved in fibroblast activation, we first examined GAS5 expression in TGF-β-treated fibroblasts. 3T3 fibroblast cells were treated with vehicle, 1, 5, or 10 ng/ml TGF-β

for 12 hours in serum free DMEM. Total RNA was extracted, and GAS5 expression was detected by RT-qPCR. As shown in Fig. 1E, GAS5 was down-regulated in TGF-β-treated 3T3 cells. TGF-β-induced GAS5 reduction was also validated in primary cultured mouse skin fibroblasts (Fig. 1F). Since fibroblast activation is an essential process leading to tissue fibrosis, and bleomycin-induced skin fibrosis involves TGF-β signaling [26-28], we assessed if GAS5 expression is altered in bleomycin-treated in skin tissues. Thus, C57BL/6 mice were injected subcutaneously with 0.02 U bleomycin daily for 14 days, skin tissues were dissected, tissue RNA was extracted, and GAS5 expression was detected by qPCR. As shown in Fig. 1G, GAS5 was indeed downregulated in fibrotic skin tissues. Moreover, we observed GAS5-expressing cells by fluorescence in situ hybridization (FISH) assay. As shown in Fig. 1H-1I, compared to the vehicle-treated skins, the numbers of GAS5-positive cells were significantly reduced in bleomycin-treated skin tissues. These results suggested that GAS5 may be involved in TGF-β-induced fibroblast activation and skin fibrosis.

GAS5 blocked TGF-β-induced fibroblast-myofibroblast transition.

Since TGF-β induces fibroblast activation through Smad3-dependent pathway and our previous studies show that GAS5 blocks TGF-β/Smad3 signaling in SMC differentiation, we sought to determine if GAS5 affects TGF-β-induced fibroblast to myofibroblast transition. Thus, we detected αSMA and Col1A protein expression in 3T3 cells transduced with AdGFP or AdGAS5 or transfected with control or GAS5 siRNA. As shown in Fig. 2A-2B, overexpression of GAS5 suppressed TGF-β-induced Col1A and αSMA protein expression. Conversely, knockdown of GAS5 by its siRNA increased TGF-β-induced Col1A and αSMA expression (Fig. 2C-2D). Consistent with the protein expression, GAS5 negatively regulated Col1A and αSMA mRNA expression (Fig. 2E-2F). Moreover, overexpression of GAS5 suppressed TGF-β-induced αSMA promoter activity (Fig. 2G). These results indicated that GAS5 inhibits TGF-β-induced fibroblast activation by negatively regulating myofibroblast marker gene transcription.

GAS5 promoted Smad3 dephosphorylation.

Previous studies have shown that TGF-β/Smad3 signaling is continuously activated or phosphorylated, which causes sustainable Smad nuclear retention during tissue fibrogenesis [40]. We have reported that Smad3 is phosphorylated and translocated into nuclei during the initial stage of TGF-β stimulation while shuttling back to cytoplasm at the later stage of TGF-β-induced smooth muscle differentiation [41]. These observations prompted us to hypothesize that GAS5 may alter Smad3 phosphorylation status/nuclear retention to regulate TGF-β-induced fibroblast activation. Since Smad3 nuclear localization depends on its phosphorylation, we tested if GAS5 affects Smad3 phosphorylation/dephosphorylation turnover in 3T3 cells by transducing the cells with control or GAS5 shRNA. As show in Fig. 3, TGF-β induced Smad3 phosphorylation. However, overexpression of GAS5 decreased Smad3 phosphorylation. These data suggest that GAS5 promoted Smad3 dephosphorylation in 3T3 cells.

GAS5 bound to Smad3 to increase Smad3 binding to PPM1A.

Smad3 phosphorylation status in the nuclei is controlled by Smad phosphatase [42-44]. To determine the mechanism by which GAS5 promotes Smad dephosphorylation, we first predicted the interactions between GAS5 and various known Smad phosphatases through lncPro (http://bioinfo.bjmu.edu.cn/lncpro/)[45]. As shown in supplementary table 1, PPM1A is the top candidate which binds GAS5. We then experimentally determined if GAS5 interacts with PPM1A and Smad3 by performing RNA immunoprecipitation (RIP) assays. RNA-protein complex from 3T3 cells were pulled down using anti-Smad3 or anti-PPM1A

antibody with IgG used as a negative control. The presence of GAS5 in the complex was detected by RT-qPCR. As shown in Fig. 4A-4B, GAS5 directly binds to Smad3 (Fig. 4A) as well as PPM1A (Fig. 4B). To characterize the function of GAS5 in Smad3-PPM1A interaction, co-immunoprecipitation (Co-IP) was performed using anti-PPM1A antibody and cell lysates isolated from 3T3 cells transduced with AdGFP/AdGAS5 or transfected with siCtrl/siGAS5. As shown in Fig. 4C-4D, overexpression of GAS5 increased Smad3-PPM1A interaction while knockdown of GAS5 suppressed Smad3-PPM1A interaction. These results indicated that GAS5 causes Smad3 dephosphorylation by promoting PPM1A binding to Smad3.

To functionally determine if GAS5 regulates myofibroblast gene expression through Smad3 pathway, we overexpressed GAS5 in 3T3 cells via adenoviral transduction along with transfection of Smad3 expression plasmid and TGF-β induction. As shown in Fig. 4E-4F, overexpression of GAS5 suppressed TGF-β-induced Col1A expression. However, Smad3 restored the Col1A expression in 3T3 cells. On the other hand, knockdown of GAS5 increased Col1A expression in 3T3 cells. But blockade of Smad3 activity by its inhibitor SIS3 demolished the effect of GAS5 knockdown on Col1A expression (Fig. 4G-4H). These results demonstrated that GAS5 negatively regulated myofibroblast gene expression by suppressing Smad3 activity, which is due to the Smad3 dephosphorylation.

GAS5 suppressed TGF-β induced fibroblast proliferation.

Fibroblast proliferation is one of the main sources for tissue mass increase during fibrosis [29, 30]. TGF-β signaling is known to regulate cell proliferation [31-33]. To confirm the function of TGF-β in fibroblast proliferation, 3T3 cells were treated with 0, 1, 5 or 10 ng/ml TGF-β for 48 hours in serum-free DMEM, following by MTT assay to assess cell proliferation. As shown in Fig. S1A, treatment of TGF-β increased 3T3 cell proliferation in a dose-dependent manner. Consistently, PCNA expression was also dose-dependent increased in response to TGF-β (Fig. S1B-1C). To determine the role of GAS5 in TGF-β-induced 3T3 proliferation, we overexpressed GAS5 by transducing 3T3 cells with control or adenoviral vector expressing GAS5 (AdGAS5) followed by treatment with vehicle or 5 ng/ml of TGF-β for 48 hours for MTT assay or 24 hours for Western blot. As shown in Figure S1D-1F, overexpression of GAS5 suppressed TGF-β-induced 3T3 proliferation (Fig. S1D) as well as PCNA protein expression (Fig. S1E-1F). On the other hand, knockdown of GAS5 by its siRNA increased 3T3 cell proliferation (Fig. S1G) and increased PCNA protein expression (Fig. S1H-1I). These results indicated that GAS5 suppressed TGF-β induced fibroblast proliferation.

GAS5 suppressed fibroblast proliferation through TGF-β/JNK signaling

It is known that TGF-β/Smad signaling cross-talks with multiple non-Smad signaling pathways, most often PI3K/Akt, JNK and p38 pathways, to regulate cell proliferation [34-39]. To determine if GAS5 inhibits fibroblast proliferation by targeting these signaling pathways, we assessed the phosphorylation of key components in PI3K/Akt, JNK and p38 signaling pathways in TGF-β-treated 3T3 cells. As shown in Supplemental Figure S2A-2B, TGF-β increased Akt and JNK phosphorylation, suggesting the activation of these signaling pathways during TGF-β-induced fibroblast proliferation. However, comparing to AdGFP-transduced cells, overexpression of GAS5 (AdGAS5) suppressed JNK phosphorylation while had no effect on p38 phosphorylation and increased the Akt phosphorylation (Fig. S2A-2B). These results suggested that GAS5 suppressed TGF-β-induced fibroblast proliferation only through JNK pathway. To further validate the function of JNK signaling in GAS5-regulated fibroblast proliferation, we knocked down GAS5 in 3T3 cells via siRNA transfection followed by treatment with vehicle or JNK pathway inhibitor, SP600125. As shown in Fig.

S2C, knockdown of GAS5 increased 3T3 cell proliferation, but treatment of JNK inhibitor reversed the effect of GAS5. These results demonstrated that GAS5 inhibits fibroblast proliferation through interfering with TGF-β-JNK pathways, in addition, to suppress fibroblast activation.

In vivo local delivery of GAS5 via adenoviral vector suppressed skin fibrosis in mice.
Since fibroblast activation is an important mechanism underlying pathological tissue/organ fibrosis, we tested the function of GAS5 in skin fibrosis by using a bleomycin-induced TGF-β-dependent skin sclerosis model [27]. GAS5 was overexpressed via adenoviral delivery in bleomycin-treated mouse skin. As shown in Fig. 5A-5D, overexpression of GAS5 attenuated bleomycin-induced skin sclerosis as indicated by the reduction of both skin thickness (Fig. 5A-5B) and skin tissue collagen deposition (Fig. 5C-5D). Immunohistochemistry (IHC) staining showed that Col1A- (Fig. 5E-5F) and αSMA-positive cells (Fig. 5G-5H) were significantly reduced in AdGAS5-transduced skin tissue, suggesting that GAS5 inhibited bleomycin-caused skin fibrosis. Moreover, overexpression of GAS5 decreased Col1A and α-SMA protein expression (Fig. 6A-6B) in bleomycin-treated skin. Importantly, GAS5 reduced the Smad3 binding to the Col1A and α-SMA promoter in a chromatin setting in vivo (Fig. 6C-6F) in the bleomycin-treated skin tissue, confirming that GAS5 impedes skin fibrogenesis by inhibiting Smad3-mediated transcription of myofibroblast genes.

Discussion

Fibrosis is a chronic wound healing progress characterized by fibroblast activation involving fibroblast proliferation and fibroblast-myofibroblast transition [46, 47]. In this study, we identified lncRNA GAS5 as an essential regulator for TGF-β-induced fibroblast activation and skin fibrosis. Specifically, GAS5 suppressed TGF-β-induced myofibroblast transition via Smad3 signaling. Mechanistically, GAS5 directly bound to both Smad3 and PPM1A, thus promoted Smad3 dephosphorylation (Fig. 7). In addition, GAS5 inhibited 3T3 cell proliferation via blocking JNK signaling. Importantly, Local adenoviral delivery of GAS5 effectively suppressed bleomycin-induced skin fibrosis in mice, suggesting that GAS5 may be used as a promising RNA based therapy for treating fibrotic diseases.

LncRNA normally functions as a suppressive protein sponge for transcription factors [22, 24]. lncRNA can also serve as a scaffold RNA which brings spatial proximity to different components thus facilitates protein complex formation and enhances their functions [48-50]. GAS5 has been shown to regulate different signaling cascades through recruiting protein co-factors to form RNA-Protein complex (RNP). Indeed, we have previously identified GAS5 as a Smad3 sponge RNA in the initial stage of TGF-β signaling transduction. In the current study, we identified a new function of GAS5 at a later stage of TGF-β signaling. I.e., GAS5 can quench the persistent TGF-β/Smad signaling observed in fibrosis by promoting PPM1A-mediated Smad3 dephosphorylation. Although transient TGF-β activity is important for tissue repair/regeneration, persistent TGF-β signaling results in fibrosis and scarring in fibrotic disease [51, 52]. Our results suggested that GAS5 may act as a brake for the persistent TGF-β signaling in tissue fibrosis. Consistently, GAS5 has been identified as an anti-fibrotic lncRNA in cardiac and hepatic fibrosis although the mechanism is mainly through functioning as miRNA sponge [53-55]. Whether GAS5 regulates TGF-β/Smad signaling in skin fibrosis through sponging miRNAs, however, requires further studies.

TGF-β not only initiates fibroblast-myofibroblast transition but also stimulates fibroblast proliferation, usually through cross-talking with Smad independent pathways, such as

PI3K/Akt, JNK and p38 [31-33]. Given the fact that GAS5 is a potent anti-proliferation lncRNA, it is not surprising that GAS5 also suppressed TGF-β-induced fibroblast proliferation. Although previous studies show that TGF-β signaling interacts with almost all major cellular signaling pathways [56], our results showed that JNK is the major downstream signaling pathway affected by GAS5 in TGF-β-induced fibroblast proliferation. There are reports showing that knockdown of GAS5 suppresses JNK phosphorylation in primary retinal ganglion cells and a neuroblastoma cell line [57, 58]. These discrepancies in GAS5 function may be due to cell type-specific effects. How GAS5 interacts with JNK signaling, and whether the interaction between GAS5 and JNK signaling is Smad3-dependent are interesting subjects for future studies.

In the progression of fibrogenesis, intensive interplays occur among different cell types. Epithelial cells, fibroblast, smooth muscle cells and immune cells all have shown to play important roles in this chronic disease [59-61]. M2 macrophages, for example, is known to play important roles not only in the initial wound healing response (anti-fibrotic) but also in the later TGF-β secretion and fibroblast activation stages (pro-fibrotic) [62]. Interestingly, GAS5 has been reported to inhibit M2 macrophage polarization [63]. Thus, GAS5 may have many unidentified functions in fibrosis. It could coordinate or modulate TGF-β signaling among different cell types during fibrogenesis. The investigation into these topics may shed new light on the RNA-based therapy in treating TGF-β-related fibrotic diseases.

Acknowledgments

This work was supported by grants from National Institutes of Health (HL123302, HL119053, HL135854, and HL147313 to S.-Y.C.).

Material and Methods:

Cells and Reagents: NIH-3T3 cells were purchased from American Type Culture Collection (ATCC). Cells were maintained at 37 °C in a humidified 5% CO2 incubator in Dulbecco's Modified Eagle's Medium (GIBCO, CA, USA) containing 10% fetal bovine serum (GIBCO, CA, USA), 100 units/ml penicillin and 100 μg/ml streptomycin. TGF-β1 was obtained from R&D Systems (Minneapolis, MN). mGAS5 siRNA (n251731) was purchased from Life Technologies (Gaithersburg, MD). Smad3 inhibitor SIS3 was purchased from Sigma-Aldrich (St. Louis, MO, USA). PPM1A (PA5–29275) antibody was purchased from ThermoFisher Scientific (Pittsburgh, PA). Akt (4691S), phospho-Akt (9271S), JNK (9252S), phospho-JNK (9251S), p38 (9212S), phospho-p38 (4511S), Smad3 (9523S), phospho-Smad3 (9520S), and Smad4 (38454) antibodies were purchased from Cell Signaling (Danvers, MA, USA). GAPDH (G8795) and α-SMA (A2547) antibodies were purchased from Sigma-Aldrich (St. Louis, MO, USA). PCNA (sc-56) and Type I Collagen (Col1A) (sc-25974) antibodies were purchased from Santa Cruz Biotechnology (Dallas, TX, USA).

Animals and skin fibrosis model: All animals were housed under conventional conditions in the animal care facility and received humane care in compliance with the Principles of Laboratory Animal Care formulated by the National Society for Medical Research and the Guide for the Care and Use of Laboratory Animals. Bleomycin-induced dermal sclerosis/fibrosis was generated following previously published protocol [27]. 8-week old male C57BL/6 mice were injected subcutaneously with 50 μg bleomycin in PBS every other day for 14 or 28 days. PBS was injected as control. Adenovirus ($1x10^8$ pfu per mouse) expressing GFP or mGAS5 was injected twice at 14 days and 28 days. After 2 or 4 weeks,

the animals were euthanized by CO2 asphyxiation. The skin areas with bleomycin injection were removed and processed for biochemical or histological analysis. All animal surgical procedures were approved by the Institutional Animal Care and Use Committee of the University of Georgia.

Quantitative RT-qPCR (qPCR): Total RNA was extracted from cells or tissues using Trizol reagent (Life Technologies, Gaithersburg, MD) and reverse-transcribed to cDNA using iScript™ cDNA Synthesis Kit (Bio-Rad, Hercules, CA). qPCR was performed using a Stratagene Mx3005 qPCR thermocycler (Agilent Technologies, La Jolla, CA). All reactions including no template controls were run in triplicates. After the reaction, the CT values were determined using fixed threshold settings. LncRNA expression was normalized to Cyclophilin (CYP).

RNA immunoprecipitation (RIP) assay: RIP assay was performed as described [24]. Cells at 80-90% confluence in 15 cm^2 culture dishes were fixed with 1% Paraformaldehyde (PFA) and lysed in FA lysis buffer (50 mM HEPES, 140 mM NaCl, 1 mM EDTA, 1% (v/v) Triton X-100, 0.1% (w/v) sodium deoxycholate, pH7.5) containing 40U/ml RNAse inhibitor (Sigma-Aldrich, St. Louis, MO) and 1X Halt™ Protease Inhibitor Cocktail (Thermofisher Scientific, Grand Island, NY). After 4–6 rounds of 50% power output sonication, 300 µl of whole cell extracts (around 500 µg total protein) were incubated with normal rabbit IgG, Smad3, Smad4, or PPM1A antibodies (1 µg) at 4°C overnight. Next day, the immune complexes were captured with protein A/G agarose beads (50 µl) (Santa Cruz Biotechnology, Dallas, TX, USA). After washing with FA lysis buffer, samples were incubated with Proteinase K at 42°C for 1 hour to digest the protein and then immunoprecipitated RNA was isolated. Purified RNA was subjected to qRT-PCR analysis for detecting the presence of GAS5.

Western blot: Cultured cells or tissue samples were lysed in RIPA buffer (50 mM Tris-HCl, pH 7.4; 150 mM NaCl; 1% NP-40; and 0.1% SDS), and incubated with continuous rotation for 10 min at 4 °C, and then centrifuged at 12 000 ×g. The supernatant was collected, and the protein concentration was determined by a BCA assay (Pierce, Rockford, USA). Protein extracts (60-100 µg) were dissolved on 10% sodium dodecyl sulfate-polyacrylamide gels (SDS-PAGE) and transferred to polyvinylidene difluoride (PVDF) membranes. The membranes were blocked with 5% non-fat milk in Tris-buffered saline (TBS) plus Tween-20 (TBST) at room temperature for 1 h followed by incubation with primary antibodies diluted in TBST at 4 °C overnight. After three 10-min washing with TBST, blots were incubated with the appropriate secondary antibody conjugated to HRP at room temperature for 1 h. The protein expression was detected with enhanced chemiluminescent reagent.

Immunofluorescent staining: Cells were seeded on coverslips placed in a 24-well plate and allowed to adhere overnight. Cells were then treated with TGF-β1 for 4 hours, fixed with 1% paraformaldehyde (PFA) in PBS, permeabilized with 0.1% Triton X-100 in PBS for 5 minutes followed by blocking with 10% goat serum and incubated with anti Smad3 antibody at 4°C overnight. Tetramethylrhodamine (TRITC)-conjugated secondary antibodies were used to detect protein expression.

Co-immunoprecipitation assay (Co-IP): Cells were transduced with Ad-GFP or Ad-GAS5 for 24 hours, and lysed with ice-cold lysis buffer containing protease inhibitor mix (Sigma). The lysates were incubated with anti-PPM1A antibody for 1 h followed by incubation with

protein A/G-beads at 4 °C for 12 h. The immunoprecipitates were pelleted, washed, and subjected to immunoblotting.

Chromatin immunoprecipitation (ChIP): Fresh tissues were minced into small pieces in ice-cold PBS with a clean razor blade. Formaldehyde was then added to a final concentration of 1% and incubated with shaking at room temperature for 10 min. The cross-linked tissues were collected by centrifugation at 4°C and washed with PBS containing protease inhibitors before final collection. The tissues were resuspended by rotating in 1% SDS lysis buffer at 4°C for 20 min followed by sonication on ice to shear DNA into 500-1000 bp fragments. The lysates were immunoprecipitated with 2 μg of IgG (negative control) or Smad3 antibody in coimmunoprecipitation reagents (17-195, Millipore). Semi-quantitative and quantitative PCR were performed to amplify α-SMA or Col1A promoter regions containing SBE.

Luciferase reporter assay: 250 ng of either empty vector or pShuttle-mGAS5 was co-transfected with 250 ng of firefly luciferase reporter driven by α-SMA promoter into 3T3 cells culured in 12-well plates using Lipofectamie LTX (Invitrogen, USA). Cells were treated with 5 ng/ml of TGF-β1 for 8 hours, and luciferase activities were measured using a luciferase assay kit (Promega) by following the manufacturer's protocol. The experiments were repeated for three times with triplicates.

Immunohistochemistry (IHC) staining: Tissue sections were rehydrated, permeabilized with 0.01% Triton X-100 in PBS, blocked with 10% goat serum, and incubated with primary antibodies at 4°C overnight followed by incubation with horseradish peroxidase (HRP)-conjugated secondary antibody. The sections were counterstained with hematoxylin.

MTT cell proliferation assay: Cell proliferation was evaluated with 3-(4,5-dimethylthiazol-2-yl)-2, 5-diphenyltetrazolium (MTT) assay using a TACS MTT Cell Proliferation Assay Kit (Trivegen). The optical density at 570 nm was measured.

Fluorescence in situ hybridization (FISH): GAS5 RNA probes (sense/antisense) were synthesized and labeled using the FISH Tag RNA Multicolor kit (Life Technologies, Gaithersburg, MD). Skin tissue cryosections were digested with 20 μg/mL proteinase K for 1 hour at 37 °C, and washed with 2 × SSC solution and with water for 5 min each at room temperature. The slides were dehydrated, air-dried and incubated with pre-denatured GAS5 probe for 24 hours at 55°C in a dark and humid environment for hybridization. Slides were washed for 4 times in 50% formamide in 2x SSC before mounting. Nuclear was counterstained with 5,6-diamidino-2-phenylindole (DAPI).

Statistical analysis: Sample or experiment sizes were determined empirically to achieve sufficient statistical power. For animal studies, the sample size was chosen to minimize the number of sacrificed animals while obtaining sufficient statistical power. In all of the experiments reported in this study, no data point was excluded. No randomization was used in this study. There was no blinding method was used to assign individuals to experimental groups. The variance is similar between groups that are being statistically compared.

Each experiment was repeated for at least three times. All values are presented as means ± SEM. Comparisons of parameters between two groups were made by two-tailed Student's t-tests. The differences among several groups will be evaluated by one-way ANOVA with Tukey-Kramer post hoc evaluation. p-values <0.05 will be considered statistically significant.

P values less than 0.05 and 0.01 were considered significant (*) or very significant (**), respectively.

Disclosures: None

Reference：

[1] W.A. Border, N.A. Noble, Transforming growth factor β in tissue fibrosis, New England Journal of Medicine, 331 (1994) 1286-1292.
[2] N.W. Todd, I.G. Luzina, S.P. Atamas, Molecular and cellular mechanisms of pulmonary fibrosis, Fibrogenesis & tissue repair, 5 (2012) 11.
[3] T.A. Wynn, Cellular and molecular mechanisms of fibrosis, The Journal of Pathology: A Journal of the Pathological Society of Great Britain and Ireland, 214 (2008) 199-210.
[4] P.L. Simonian, C.L. Roark, F. Wehrmann, A.K. Lanham, F.D. del Valle, W.K. Born, R.L. O'Brien, A.P. Fontenot, Th17-polarized immune response in a murine model of hypersensitivity pneumonitis and lung fibrosis, The Journal of Immunology, 182 (2009) 657-665.
[5] I.G. Luzina, N.W. Todd, A.T. Iacono, S.P. Atamas, Roles of T lymphocytes in pulmonary fibrosis, Journal of leukocyte biology, 83 (2008) 237-244.
[6] F. Huaux, T. Liu, B. McGarry, M. Ullenbruch, Z. Xing, S.H. Phan, Eosinophils and T lymphocytes possess distinct roles in bleomycin-induced lung injury and fibrosis, The Journal of Immunology, 171 (2003) 5470-5481.
[7] T.L. Bonfield, J.R. Panuska, M.W. Konstan, K.A. Hilliard, J.B. Hilliard, H. Ghnaim, M. Berger, Inflammatory cytokines in cystic fibrosis lungs, American journal of respiratory and critical care medicine, 152 (1995) 2111-2118.
[8] F. Heymann, C. Trautwein, F. Tacke, Monocytes and macrophages as cellular targets in liver fibrosis, Inflammation & Allergy-Drug Targets (Formerly Current Drug Targets-Inflammation & Allergy), 8 (2009) 307-318.
[9] M. Pedroza, T.T. Le, K. Lewis, H. Karmouty-Quintana, S. To, A.T. George, M.R. Blackburn, D.J. Tweardy, S.K. Agarwal, STAT-3 contributes to pulmonary fibrosis through epithelial injury and fibroblast-myofibroblast differentiation, The FASEB Journal, 30 (2015) 129-140.
[10] S.H. Phan, The myofibroblast in pulmonary fibrosis, Chest, 122 (2002) 286S-289S.
[11] M. Zeisberg, G. Bonner, Y. Maeshima, P. Colorado, G.A. Müller, F. Strutz, R. Kalluri, Renal fibrosis: collagen composition and assembly regulates epithelial-mesenchymal transdifferentiation, The American journal of pathology, 159 (2001) 1313-1321.
[12] E.M. Zeisberg, S.E. Potenta, H. Sugimoto, M. Zeisberg, R. Kalluri, Fibroblasts in kidney fibrosis emerge via endothelial-to-mesenchymal transition, Journal of the American Society of Nephrology, 19 (2008) 2282-2287.
[13] J. Massagué, Y.-G. Chen, Controlling TGF-β signaling, Genes & development, 14 (2000) 627-644.
[14] K. Miyazono, TGF-β signaling by Smad proteins, Cytokine & growth factor reviews, 11 (2000) 15-22.
[15] A. Leask, D.J. Abraham, TGF-β signaling and the fibrotic response, The FASEB Journal, 18 (2004) 816-827.
[16] A. Biernacka, M. Dobaczewski, N.G. Frangogiannis, TGF-β signaling in fibrosis, Growth factors, 29 (2011) 196-202.
[17] R. Derynck, Y.E. Zhang, Smad-dependent and Smad-independent pathways in TGF-β family signalling, Nature, 425 (2003) 577.

[18] Y.E. Zhang, Non-Smad pathways in TGF-β signaling, Cell research, 19 (2009) 128.
[19] L. Koch, Functional genomics: screening for lncRNA function, Nature Reviews Genetics, 18 (2017) 70.
[20] T.R. Mercer, J.S. Mattick, Structure and function of long noncoding RNAs in epigenetic regulation, Nature structural & molecular biology, 20 (2013) 300.
[21] M. Huarte, The emerging role of lncRNAs in cancer, Nature medicine, 21 (2015) 1253.
[22] T. Kino, D.E. Hurt, T. Ichijo, N. Nader, G.P. Chrousos, Noncoding RNA gas5 is a growth arrest–and starvation-associated repressor of the glucocorticoid receptor, Sci. Signal., 3 (2010) ra8-ra8.
[23] M. Mourtada-Maarabouni, M. Pickard, V. Hedge, F. Farzaneh, G. Williams, GAS5, a non-protein-coding RNA, controls apoptosis and is downregulated in breast cancer, Oncogene, 28 (2009) 195.
[24] R. Tang, G. Zhang, Y.-C. Wang, X. Mei, S.-Y. Chen, The long non-coding RNA GAS5 regulates transforming growth factor β (TGF-β)–induced smooth muscle cell differentiation via RNA Smad–binding elements, Journal of Biological Chemistry, 292 (2017) 14270-14278.
[25] R. Tang, X. Mei, Y.-C. Wang, X.-B. Cui, G. Zhang, W. Li, S.-Y. Chen, LncRNA GAS5 regulates vascular smooth muscle cell cycle arrest and apoptosis via p53 pathway, Biochimica et Biophysica Acta (BBA)-Molecular Basis of Disease, 1865 (2019) 2516-2525.
[26] C.E. Daniels, M.C. Wilkes, M. Edens, T.J. Kottom, S.J. Murphy, A.H. Limper, E.B. Leof, Imatinib mesylate inhibits the profibrogenic activity of TGF-β and prevents bleomycin-mediated lung fibrosis, The Journal of clinical investigation, 114 (2004) 1308-1316.
[27] C. Sun, S.-Y. Chen, RGC32 promotes bleomycin-induced systemic sclerosis in a murine disease model by modulating classically activated macrophage function, The Journal of Immunology, 200 (2018) 2777-2785.
[28] S.N. Giri, D.M. Hyde, M.A. Hollinger, Effect of antibody to transforming growth factor beta on bleomycin induced accumulation of lung collagen in mice, Thorax, 48 (1993) 959-966.
[29] E. Garbuzenko, A. Nagler, D. Pickholtz, P. Gillery, R. Reich, F.X. Maquart, F. Levi-Schaffer, Human mast cells stimulate fibroblast proliferation, collagen synthesis and lattice contraction: a direct role for mast cells in skin fibrosis, Clinical & Experimental Allergy, 32 (2002) 237-246.
[30] T.J. Daly, W.L. Weston, Retinoid effects on fibroblast proliferation and collagen synthesis in vitro and on fibrotic disease in vivo, Journal of the American Academy of Dermatology, 15 (1986) 900-902.
[31] D.A. Bettinger, D.R. Yager, R.F. Diegelmann, I.K. Cohen, The effect of TGF-beta on keloid fibroblast proliferation and collagen synthesis, Plastic and reconstructive surgery, 98 (1996) 827-833.
[32] N. Abdullah, B. Torres, M. Basu, H. Johnson, Differential effects of epidermal growth factor, transforming growth factor-alpha, and vaccinia virus growth factor in the positive regulation of IFN-gamma production, The Journal of Immunology, 143 (1989) 113-117.
[33] W.-Y. Huang, Z.-G. Li, H. Rus, X. Wang, P.A. Jose, S.-Y. Chen, RGC-32 mediates transforming growth factor-β-induced epithelial-mesenchymal transition in human renal proximal tubular cells, Journal of Biological Chemistry, 284 (2009) 9426-9432.
[34] E.J. Battegay, E.W. Raines, R.A. Seifert, D.F. Bowen-Pope, R. Ross, TGF-β induces bimodal proliferation of connective tissue cells via complex control of an autocrine PDGF loop, Cell, 63 (1990) 515-524.
[35] S.S. Huang, J.S. Huang, TGF-β control of cell proliferation, Journal of cellular biochemistry, 96 (2005) 447-462.
[36] Y.E. Zhang, Non-Smad pathways in TGF-β signaling, Cell research, 19 (2009) 128-139.

[37] K. Song, H. Wang, T.L. Krebs, D. Danielpour, Novel roles of Akt and mTOR in suppressing TGF-β/ALK5-mediated Smad3 activation, The EMBO journal, 25 (2006) 58-69.
[38] M.E. Engel, M.A. McDonnell, B.K. Law, H.L. Moses, Interdependent SMAD and JNK signaling in transforming growth factor-β-mediated transcription, Journal of Biological Chemistry, 274 (1999) 37413-37420.
[39] A.V. Bakin, C. Rinehart, A.K. Tomlinson, C.L. Arteaga, p38 mitogen-activated protein kinase is required for TGFβ-mediated fibroblastic transdifferentiation and cell migration, Journal of cell science, 115 (2002) 3193-3206.
[40] S. Takagawa, G. Lakos, Y. Mori, J. Varga, T. Yamamoto, K. Nishioka, Sustained activation of fibroblast transforming growth factor-β/Smad signaling in a murine model of scleroderma, Journal of investigative dermatology, 121 (2003) 41-50.
[41] W.-B. Xie, Z. Li, J.M. Miano, X. Long, S.-Y. Chen, Smad3-mediated Myocardin Silencing A NOVEL MECHANISM GOVERNING THE INITIATION OF SMOOTH MUSCLE DIFFERENTIATION, Journal of Biological Chemistry, 286 (2011) 15050-15057.
[42] K. Dong, X. Guo, W. Chen, A.C. Hsu, Q. Shao, J.-F. Chen, S.-Y. Chen, Mesenchyme homeobox 1 mediates transforming growth factor-β (TGF-β)–induced smooth muscle cell differentiation from mouse mesenchymal progenitors, Journal of Biological Chemistry, 293 (2018) 8712-8719.
[43] B. Bourgeois, B. Gilquin, C. Tellier-Lebègue, C. Östlund, W. Wu, J. Pérez, P. El Hage, F. Lallemand, H.J. Worman, S. Zinn-Justin, Inhibition of TGF-β signaling at the nuclear envelope: characterization of interactions between MAN1, Smad2 and Smad3, and PPM1A, Sci. Signal., 6 (2013) ra49-ra49.
[44] D.L. Bruce, G.P. Sapkota, Phosphatases in SMAD regulation, FEBS letters, 586 (2012) 1897-1905.
[45] Q. Lu, S. Ren, M. Lu, Y. Zhang, D. Zhu, X. Zhang, T. Li, Computational prediction of associations between long non-coding RNAs and proteins, BMC genomics, 14 (2013) 651.
[46] G.R. Grotendorst, H. Rahmanie, M.R. Duncan, Combinatorial signaling pathways determine fibroblast proliferation and myofibroblast differentiation, The FASEB Journal, 18 (2004) 469-479.
[47] F. Strutz, M. Zeisberg, Renal fibroblasts and myofibroblasts in chronic kidney disease, Journal of the American Society of Nephrology, 17 (2006) 2992-2998.
[48] R. Tang, X. Mei, Y.-C. Wang, X.-B. Cui, G. Zhang, W. Li, S.-Y. Chen, LncRNA GAS5 regulates vascular smooth muscle cell cycle arrest and apoptosis via p53 pathway, Biochimica et Biophysica Acta (BBA)-Molecular Basis of Disease, (2019).
[49] K.C. Wang, H.Y. Chang, Molecular mechanisms of long noncoding RNAs, Molecular cell, 43 (2011) 904-914.
[50] M. Sun, F. Nie, Y. Wang, Z. Zhang, J. Hou, D. He, M. Xie, L. Xu, W. De, Z. Wang, LncRNA HOXA11-AS promotes proliferation and invasion of gastric cancer by scaffolding the chromatin modification factors PRC2, LSD1, and DNMT1, Cancer research, 76 (2016) 6299-6310.
[51] K.R. Cutroneo, TGF-β–induced fibrosis and SMAD signaling: oligo decoys as natural therapeutics for inhibition of tissue fibrosis and scarring, Wound Repair and Regeneration, 15 (2007) S54-S60.
[52] A. Leask, C.P. Denton, D.J. Abraham, Insights into the molecular mechanism of chronic fibrosis: the role of connective tissue growth factor in scleroderma, Journal of Investigative Dermatology, 122 (2004) 1-6.
[53] H. Tao, J.-G. Zhang, R.-H. Qin, C. Dai, P. Shi, J.-J. Yang, Z.-Y. Deng, K.-H. Shi, LncRNA GAS5 controls cardiac fibroblast activation and fibrosis by targeting miR-21 via PTEN/MMP-2 signaling pathway, Toxicology, 386 (2017) 11-18.

[54] F. Yu, J. Zheng, Y. Mao, P. Dong, Z. Lu, G. Li, C. Guo, Z. Liu, X. Fan, Long non-coding RNA growth arrest-specific transcript 5 (GAS5) inhibits liver fibrogenesis through a mechanism of competing endogenous RNA, Journal of Biological Chemistry, 290 (2015) 28286-28298.
[55] Z. Dong, S. Li, X. Wang, L. Si, R. Ma, L. Bao, A. Bo, lncRNA GAS5 restrains CCl4-induced hepatic fibrosis by targeting miR-23a through the PTEN/PI3K/Akt signaling pathway, American Journal of Physiology-Gastrointestinal and Liver Physiology, 316 (2019) G539-G550.
[56] L. Xiao, Y. Du, Y. Shen, Y. He, H. Zhao, Z. Li, TGF-beta 1 induced fibroblast proliferation is mediated by the FGF-2/ERK pathway, Front Biosci (Landmark Ed), 17 (2012) 2667-2674.
[57] X. Miao, A. Liang, Knockdown of long noncoding RNA GAS5 attenuates H2O2-induced damage in retinal ganglion cells through upregulating miR-124: Potential role in traumatic brain injury, Journal of cellular biochemistry, 120 (2019) 2313-2322.
[58] X.-B. Zhou, L.-F. Lai, G.-B. Xie, C. Ding, X. Xu, Y. Wang, LncRNA GAS5 sponges miRNA-221 to promote neurons apoptosis by up-regulated PUMA under hypoxia condition, Neurological Research, (2019) 1-9.
[59] T. Krieg, D. Abraham, R. Lafyatis, Fibrosis in connective tissue disease: the role of the myofibroblast and fibroblast-epithelial cell interactions, Arthritis research & therapy, 9 (2007) S4.
[60] N. Sakai, A.M. Tager, Fibrosis of two: Epithelial cell-fibroblast interactions in pulmonary fibrosis, Biochimica et Biophysica Acta (BBA)-Molecular Basis of Disease, 1832 (2013) 911-921.
[61] S. Hays, R. Ferrando, R. Carter, H. Wong, P. Woodruff, Structural changes to airway smooth muscle in cystic fibrosis, Thorax, 60 (2005) 226-228.
[62] T.T. Braga, J.S.H. Agudelo, N.O.S. Camara, Macrophages during the fibrotic process: M2 as friend and foe, Frontiers in immunology, 6 (2015) 602.
[63] D. Sun, Z. Yu, X. Fang, M. Liu, Y. Pu, Q. Shao, D. Wang, X. Zhao, A. Huang, Z. Xiang, LncRNA GAS5 inhibits microglial M2 polarization and exacerbates demyelination, EMBO reports, 18 (2017) 1801-1816.

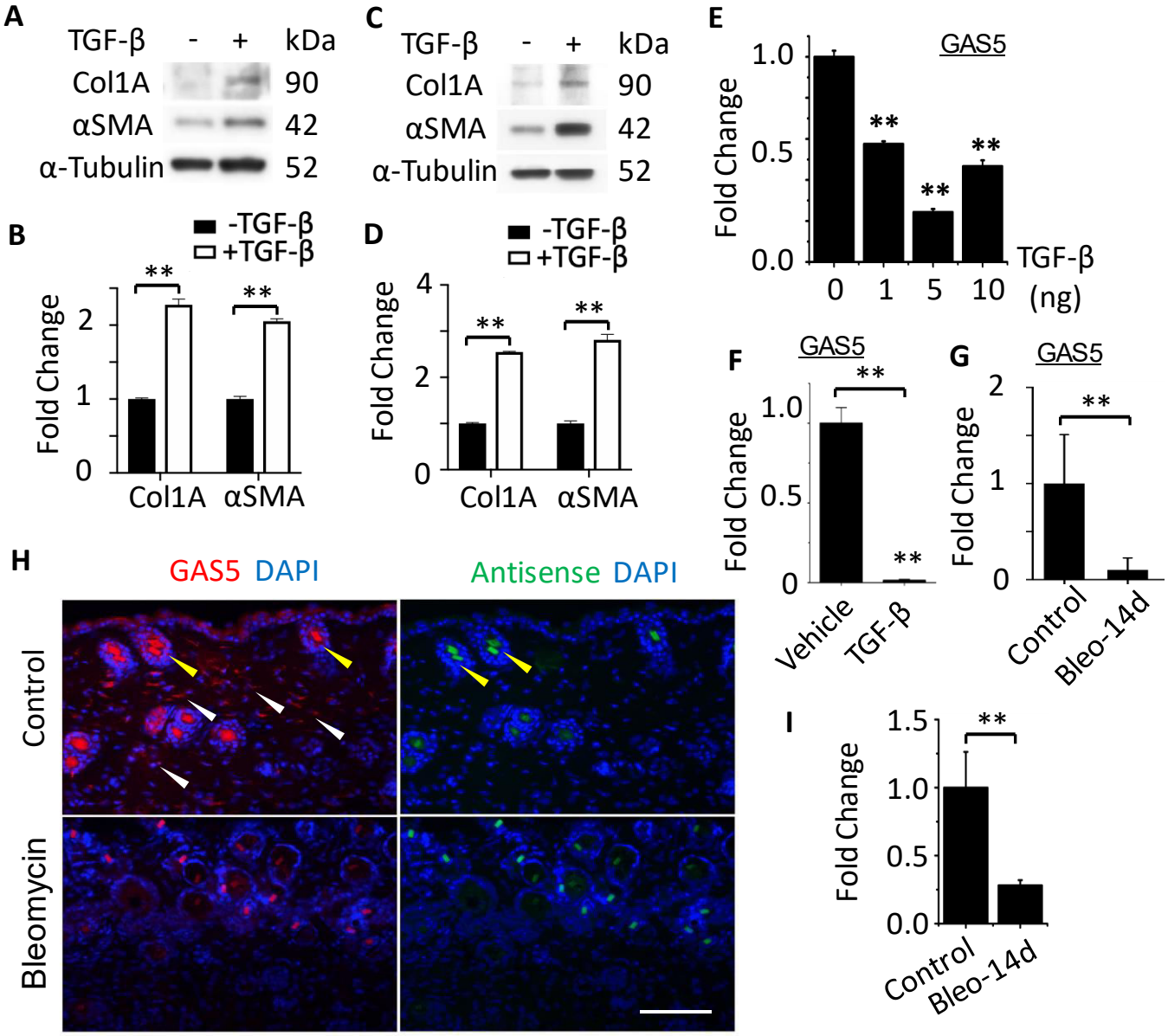

Figure 1: LncRNA GAS5 was downregulated in fibroblasts by TGF-β. A-D), TGF-β (5ng/ml) induced the expression of myofibroblast cell marker Col1A and α-SMA in 3T3 fibroblasts (A-B) and primary skin fibroblasts (C-D). **B)** Quantification of protein expression in **A** by normalizing to α-Tubulin. **D)** Quantification of protein expression in **C** by normalizing to α-Tubulin. **E)** TGF-β down-regulated GAS5 in 3T3 fibroblasts in a dose dependent manner. 3T3 fibroblast cells were cultured in serum free DMEM medium with 0, 1, 5, 10 ng/ml of TGF-β for 12 hrs. **F)** TGF-β (5ng/ml) down-regulated GAS5 in primary mouse skin fibroblasts. **G)** GAS5 was down-regulated in skin tissues with bleomycin treatment, as analyzed by RT-qPCR. C57BL/6 mice were injected subcutaneously with bleomycin (Bleo; 0.02 U) daily for 14 days. GAS5 RNA expression was calculated by normalizing to cyclophilin mRNA. **H)** GAS5 positive cells in skin tissues were decreased by bleomycin treatment. Skin tissues from (G) was fixed in 4% PFA, and GAS5 positive cells were shown by RNA-FISH staining. Positive stain (white arrow), and false positive stain (yellow arrow) were indicated by arrows **I)** Quantification of **GAS-positive cells** by counting the positive staining from 10 different fields, shown as fold change. Bar: 200µm. * $p<0.05$; ** $p<0.01$; n=3.

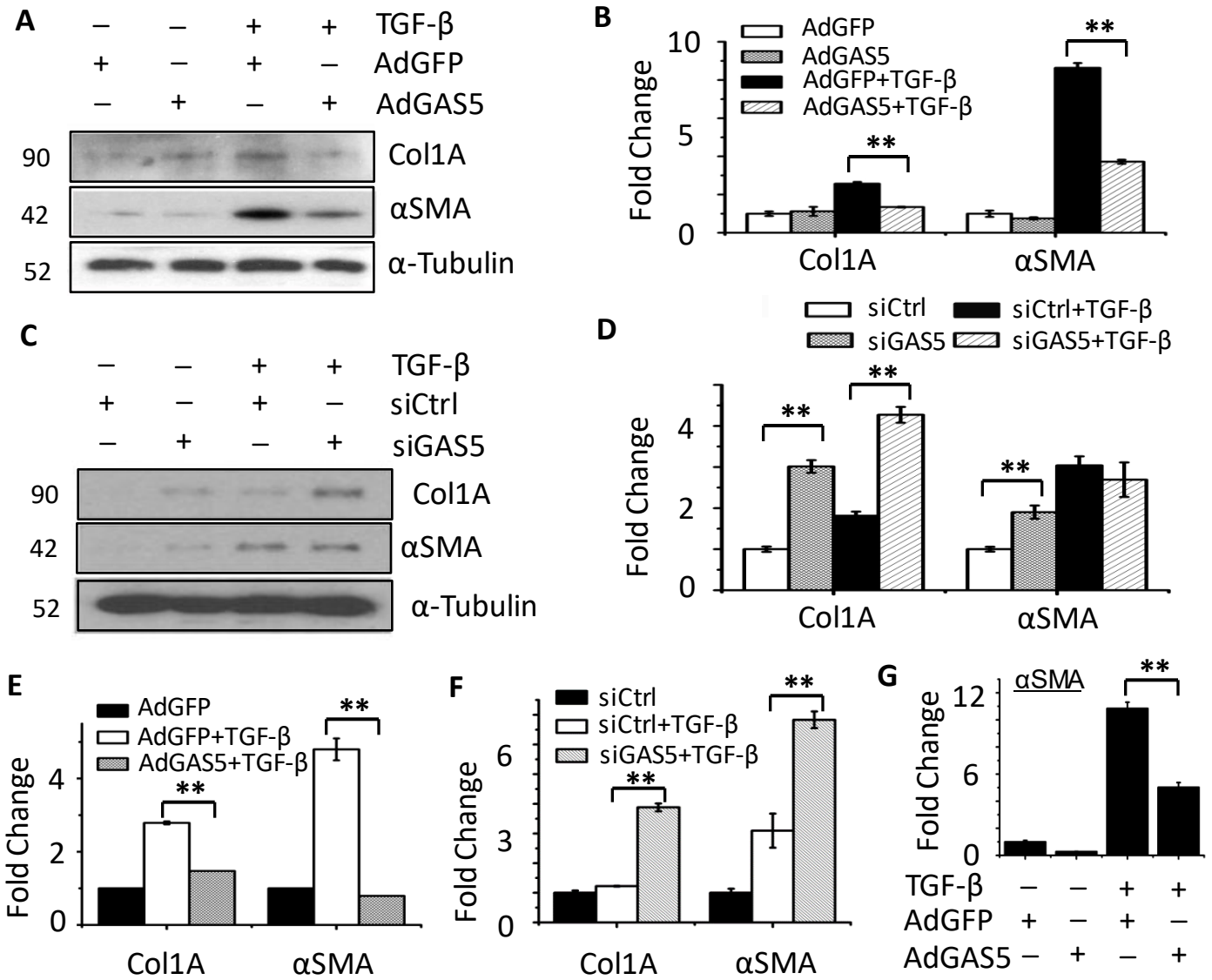

Figure 2. GAS5 suppressed TGF-β-induced fibroblast-myofibroblast transition. A-B) GAS5 suppressed αSMA and Col1A protein expression. 3T3 cells were transduced with AdGFP or AdGAS5 followed by vehicle or 5 ng/ml of TGF-β treatment for 24 hrs. αSMA and Col1A expression was assessed by Western blot (A) and quantified by normalizing to α-Tubulin (B). **C-D)** Knockdown of GAS5 increased αSMA and Col1A protein expression. 3T3 cells were transfected with siCtrl or siGAS5 followed by vehicle or 5 ng/ml of TGF-β treatment for 24 hrs. αSMA and Col1A expression was assessed by Western blot (C) and quantified by normalizing to α-Tubulin (D). **E)** GAS5 suppressed TGF-β-induced mRNA expression of αSMA and Col1A. 3T3 cells were transduced with AdGFP or AdGAS5 followed by vehicle or 5 ng/ml of TGF-β treatment for 12 hrs. mRNA expression was assessed by RT-qPCR and normalized to cyclophilin. **F)** Knockdown of GAS5 increased mRNA expression of αSMA and Col1A. 3T3 cells were transfected with siCtrl or siGAS5 followed by vehicle or 5 ng/ml of TGF-β treatment for 12 hrs. mRNA expression was assessed by qPCR and normalized to cyclophilin. **G)** GAS5 suppressed TGF-β-induced αSMA promoter activity. 3T3 cells were transduced with AdGFP or AdGAS5 and transfected with αSMA promoter luciferase reporter for 24 hours prior to the treatment with vehicle or 5 ng/ml of TGF-β for 8 hours. Luciferase assays were performed. * $p<0.05$; ** $p<0.01$; n=3.

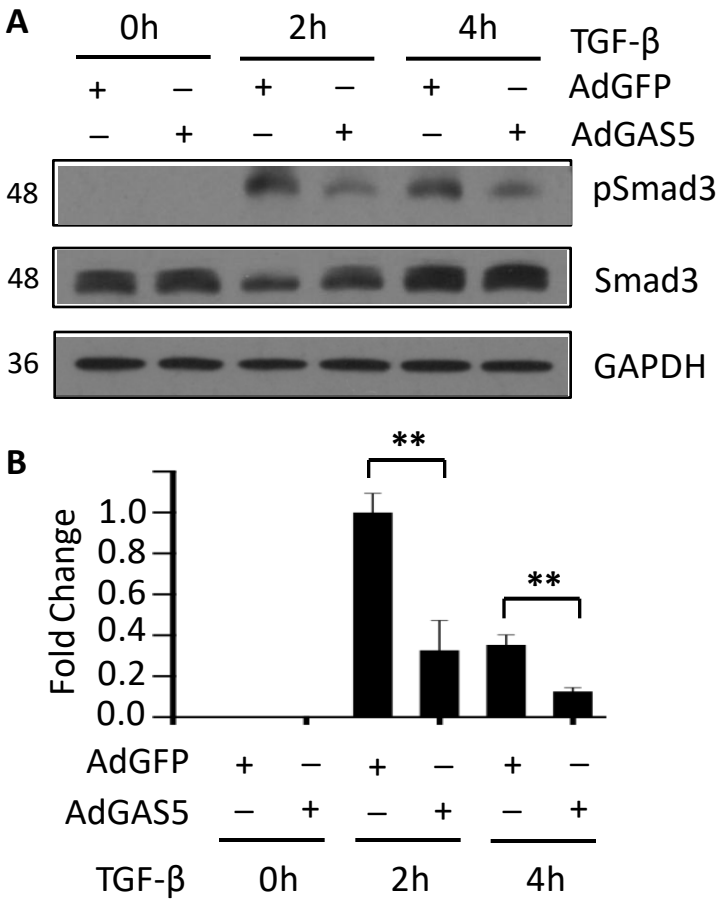

Figure 3. GAS5 promoted Smad3 dephosphorylation. A) GAS5 accelerated Smad3 dephosphorylation in TGF-β-treated fibroblasts. 3T3 cells were transduced with AdGFP or AdGAS5 followed by vehicle (0 h) or 5 ng/ml of TGF-β treatment for 2 or 4 h. Phospho- and total Smad3 were detected by Western blot. **B)** Phospho-Smad3 was quantified by normalizing to the total Smad3. ** $p<0.01$; n=3.

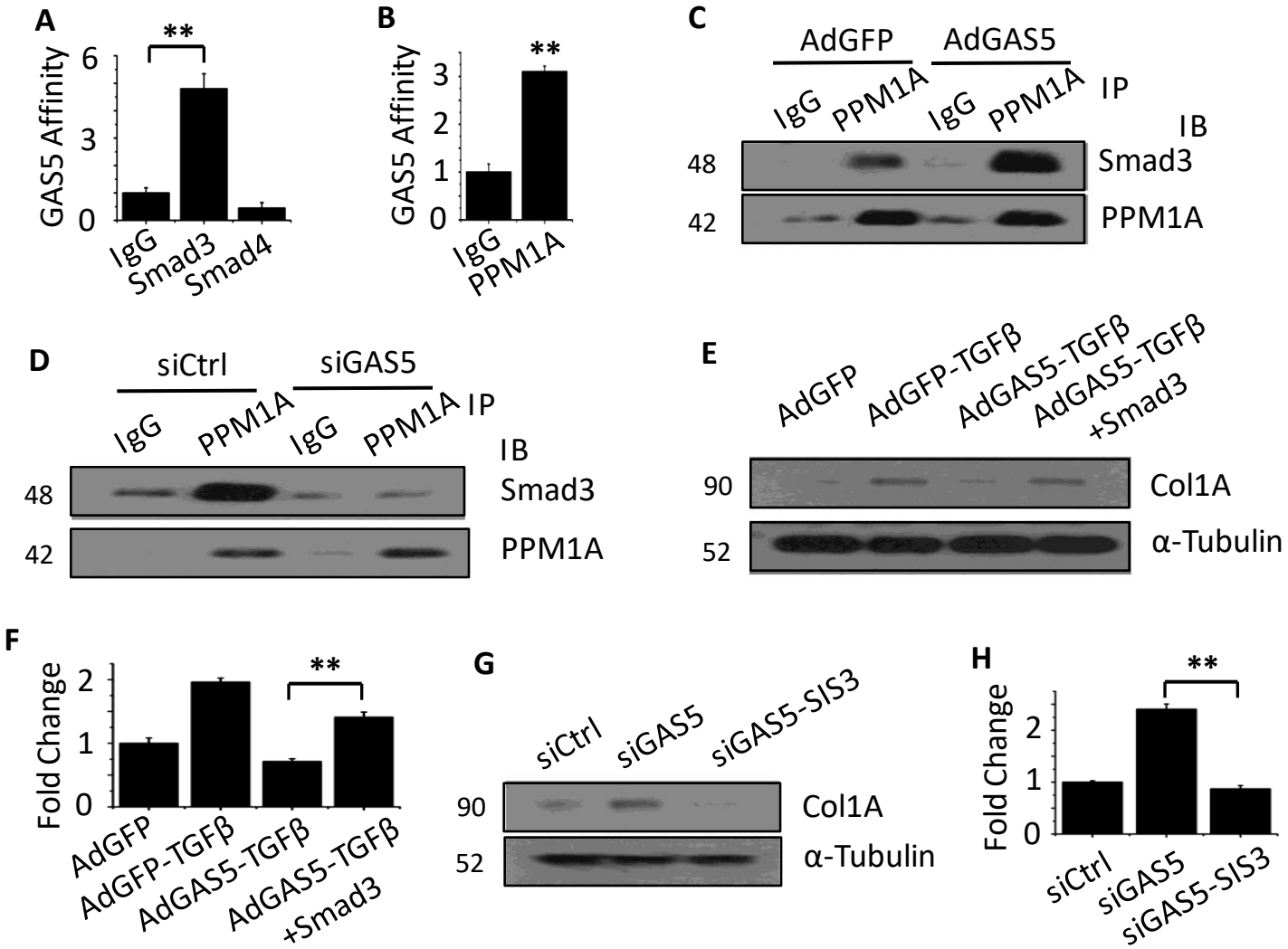

Figure 4. GAS5 enhanced PPM1A binding affinity to Smad3. A) GAS5 bound to Smad3 as shown by RIP assay. Smad3- and Smad4-interacting molecules in 3T3 cells were pulled down by their antibodies, respectively. The presence of GAS5 was detected via qPCR. **B)** GAS5 bound PPM1A in 3T3 fibroblasts. PPM1A-interacting molecules in 3T3 cells was pulled down by its antibody, and the presence of GAS5 was detected by qPCR. **C-D)** Over expression of GAS5 promoted while Knockdown of GAS5 suppressed Smad3-PPM1A interaction. 3T3 cells were transduced with AdGFP or AdGAS5 (C) or transfected with siCtrl or siGAS5 (D) as indicated for 24 h. Co-immunoprecipitation was preformed by using PPM1A antibody, and the presence of Smad3 was detected by Western blot. **E-F)** Overexpression of Smad3 restored GAS5-blocked Col1A expression. 3T3 cells were transduced with AdGFP or AdGAS5 and transfected with control or Smad3 expression plasmid followed by treatment with 5 ng/ml of TGF-β for 24 hours. Col1A expression was assessed by Western blot (E) and quantified by normalizing to α-Tubulin (F). **G-H)** Smad3 inhibitor SIS3 blunted GAS5 knockdown-enhanced Col1A expression. 3T3 cells were transfected with siCtrl or siGAS5 followed by vehicle or SIS3 (10 μM) treatment for 24 hours. Col1A expression was assessed by Western blot (G) and quantified by normalizing to α-Tubulin (H). * $p<0.05$; ** $p<0.01$; n=3.

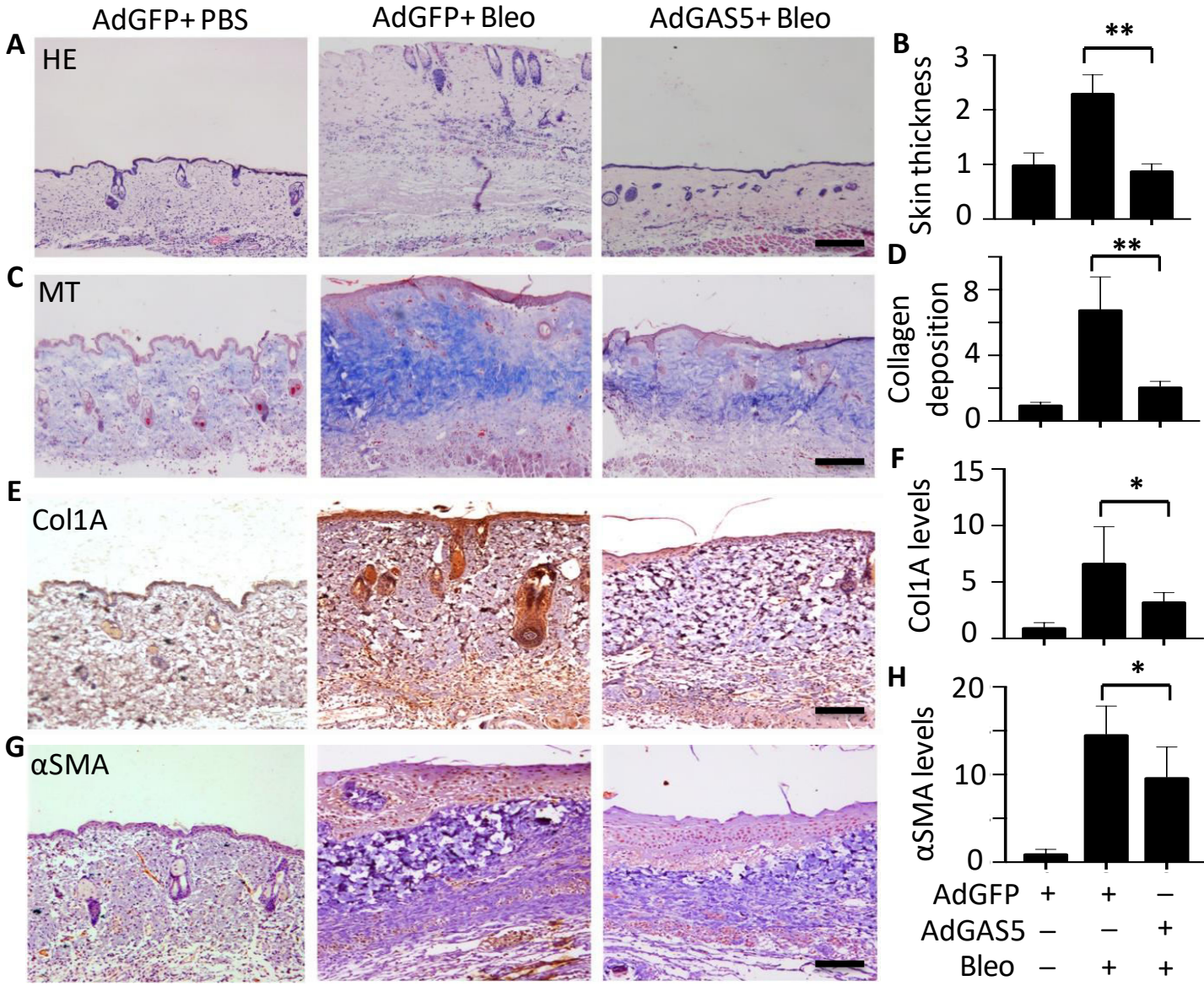

Figure 5. GAS5 suppressed skin fibrosis in mice. A-D) Forced expression of GAS5 via local adenoviral delivery suppressed bleomycin (0.02U)-induced skin fibrosis in mice. Mouse skins were treated with bleomycin for 28 days. The skin tissues were stained with H&E for structural changes (A), Masson's trichrome (MT) for collagen deposition (C). Bar: 400 µm. Skin thicknesses shown in A were averaged from 10 different fields (B), and collagen deposition in C was quantified by measuring the staining intensity from 10 different fields (D). **E-H)** Forced expression of GAS5 via local adenoviral delivery suppressed bleomycin-induced expression of Col1A (E-F) and αSMA (G-H). Skin tissue sections underwent immunohistochemistry (IHC) staining using Col1A (E) and αSMA (G) antibodies, respectively. Col1A (F) and αSMA (H)-positive cells were averaged from 10 different fields. Bar: 400 µm. * $p<0.05$; ** $p<0.01$; n=5.

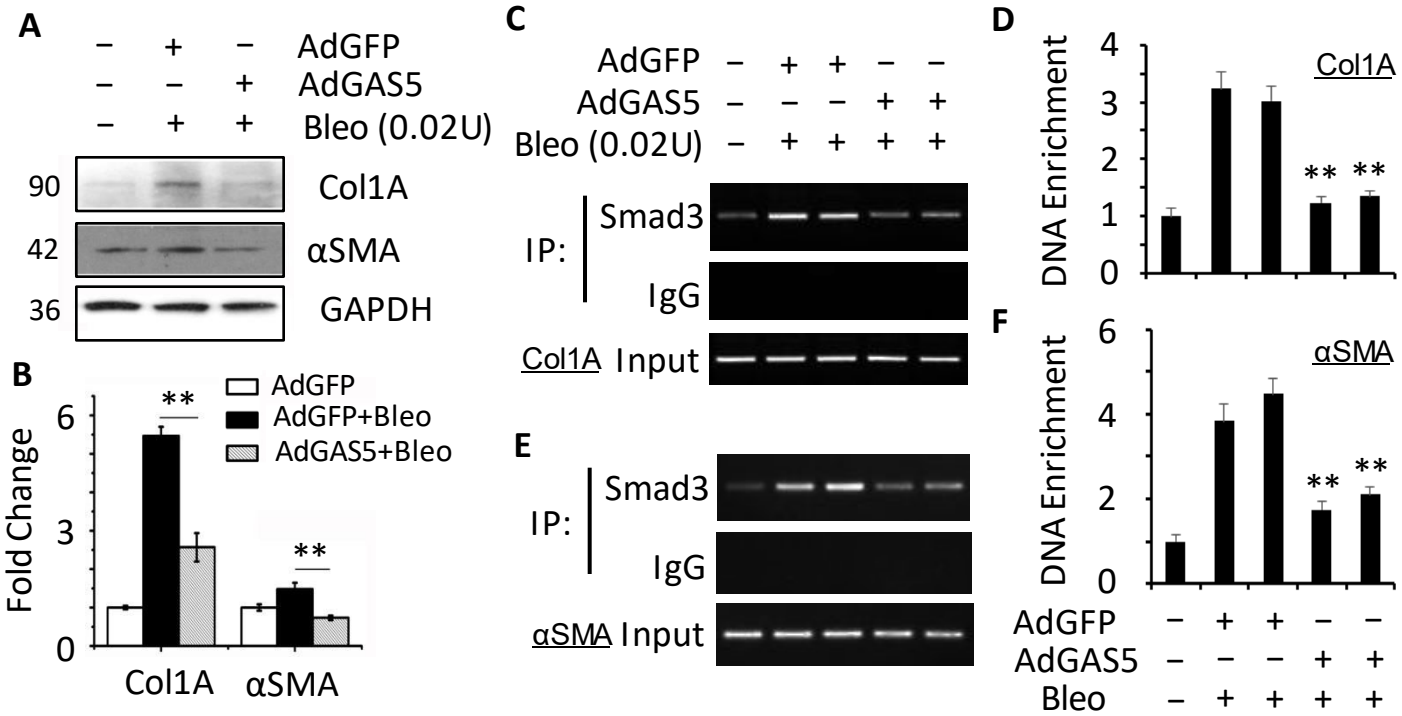

Figure 6. GAS5 inhibited Col1A and αSMA protein expression in fibrotic skin tissues and attenuated Smad3 binding to their promoters in vivo. A) GAS5 suppressed Col1A and αSMA protein expression in skin tissues with bleomycin-induced fibrosis. **B)** Col1a and αSMA protein levels in (A) were quantified by normalizing to GAPDH. **C-F)** GAS5 suppressed Smad3 binding to Col1a (C-D) and α-SMA (E-F) promoters in vivo that were significantly enriched during bleomycin-induced skin fibrosis. Smad3 binding to Col1a (C) and α-SMA (E) promoters in a chromatin setting was measured by in vivo chromatin immunoprecipitation (CHIP) assay. Smad3 binding enrichments were quantified by qPCR relative to the Smad3 binding in vehicle-treated skin tissues (D-F).

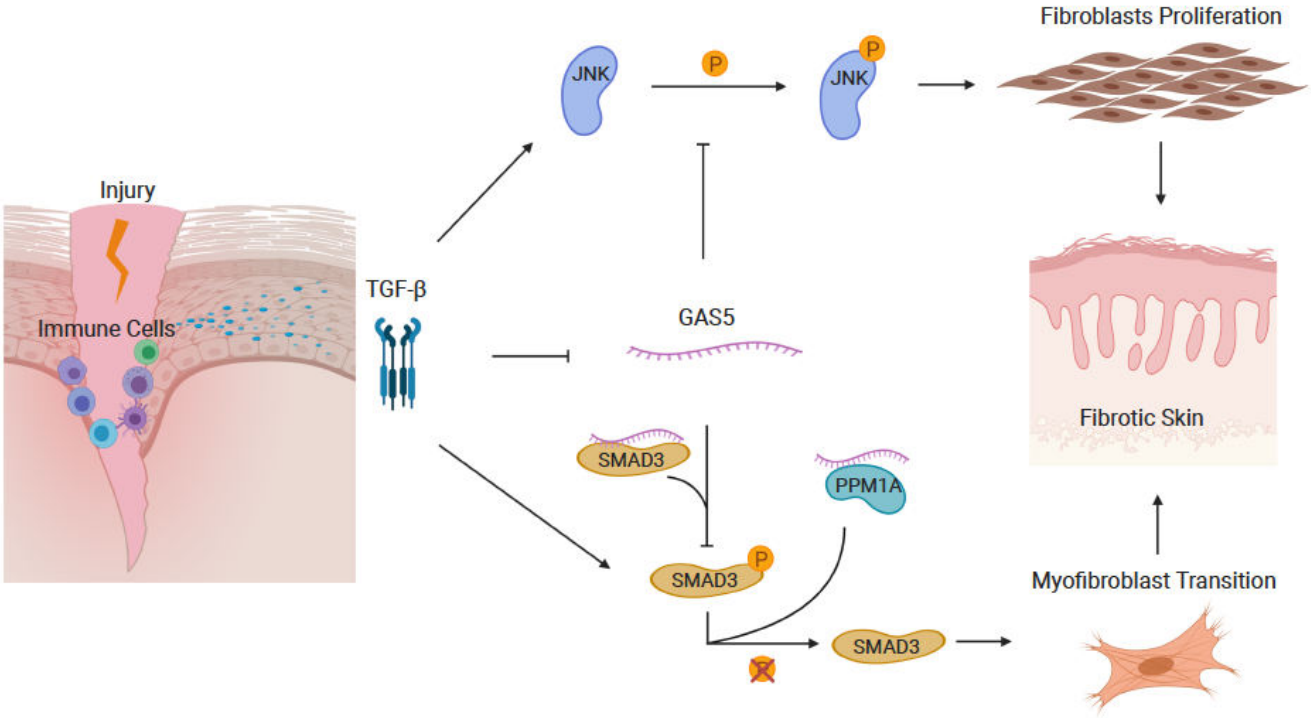

Figure 7. A diagram of GAS5 in TGF-β-induced skin fibrosis. During the onset of skin fibrosis, infiltrating immune cells secret TGF-β, which activates resident fibroblasts through Smad3 pathway. GAS5 suppresses the progression of fibrosis by promoting Smad3 dephosphorylation through facilitating PPM1A binding to Smad3, thus inhibiting Smad3-mediated myofibroblast activation. GAS5 also inhibits fibroblast proliferation through impeding JNK signaling pathway.

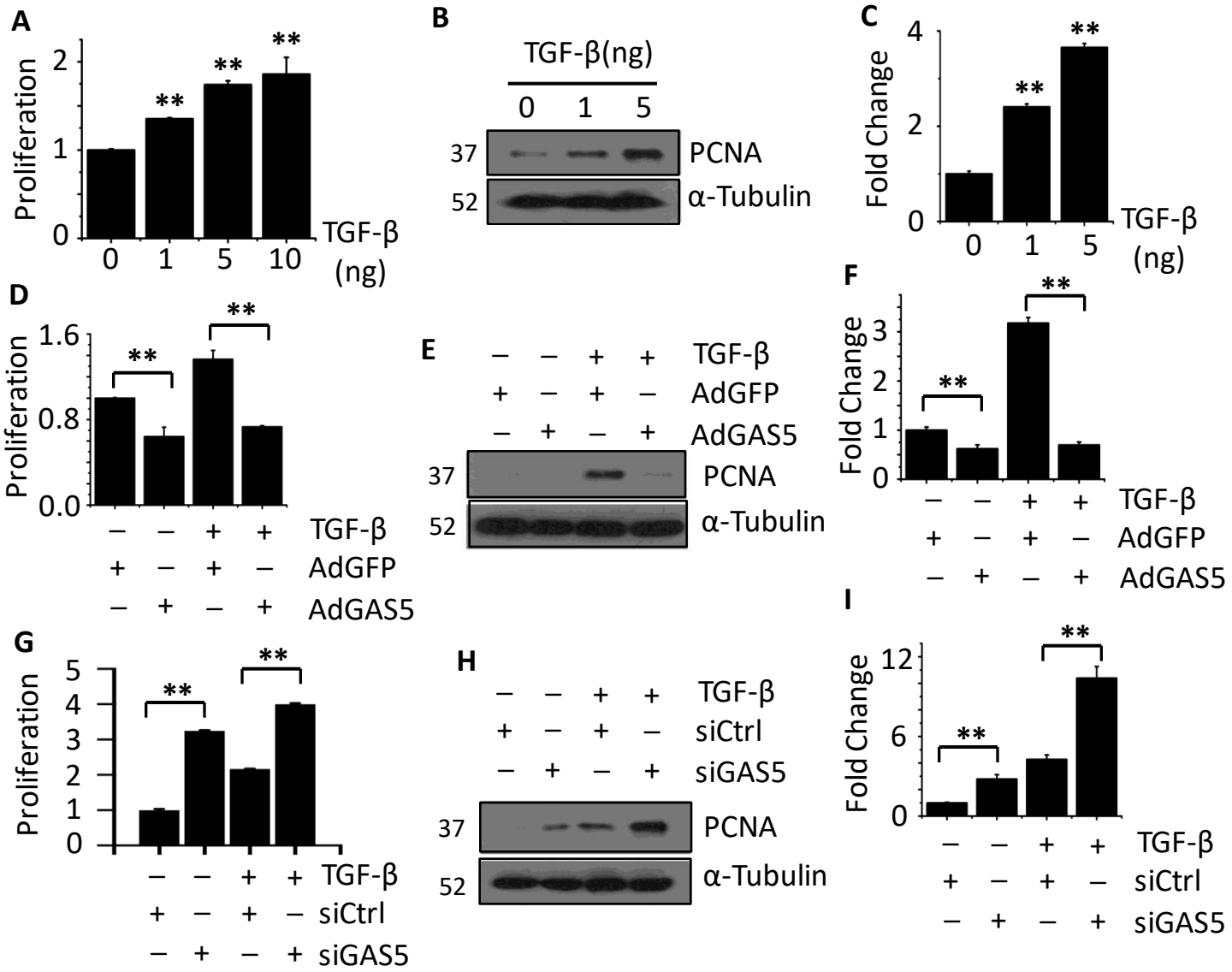

Supplemental Figure S1. GAS5 suppressed TGF-β induced fibroblast proliferation. A) TGF-β induced 3T3 fibroblast proliferation in a dose-dependent manner. Cell proliferation rate was assessed by MTT assay and compared to the untreated cells (0 ng/ml). **B)** TGF-β induced PCNA expression in a dose-dependent manner in 3T3 cells. **C)** Quantification of **PCNA levels** by normalizing to α-Tubulin. **D-F)** Overexpression of GAS5 suppressed TGF-β-induced 3T3 cell proliferation and PCNA expression. 3T3 cells were transduced with AdGFP or AdGAS5 for 24 hrs and then cultured in DMEM with 10% FBS with vehicle or TGF-β (5 ng/ml) treatment for 48 hrs. Cell proliferation was assessed by MTT assay. **E)** PCNA expression was detected by Western blot and quantified by normalizing to α-Tubulin as in (F). **G-I)** Knockdown of GAS5 promoted 3T3 proliferation and PCNA expression. 3T3 cells were transfected with siCtrl or siGAS5 for 24 hrs followed by treatment with vehicle or 5 ng/ml of TGF-β for 48 hrs. Cell proliferation and PCNA expression were assessed as in (D-F). * $p<0.05$; ** $p<0.01$; n=3.

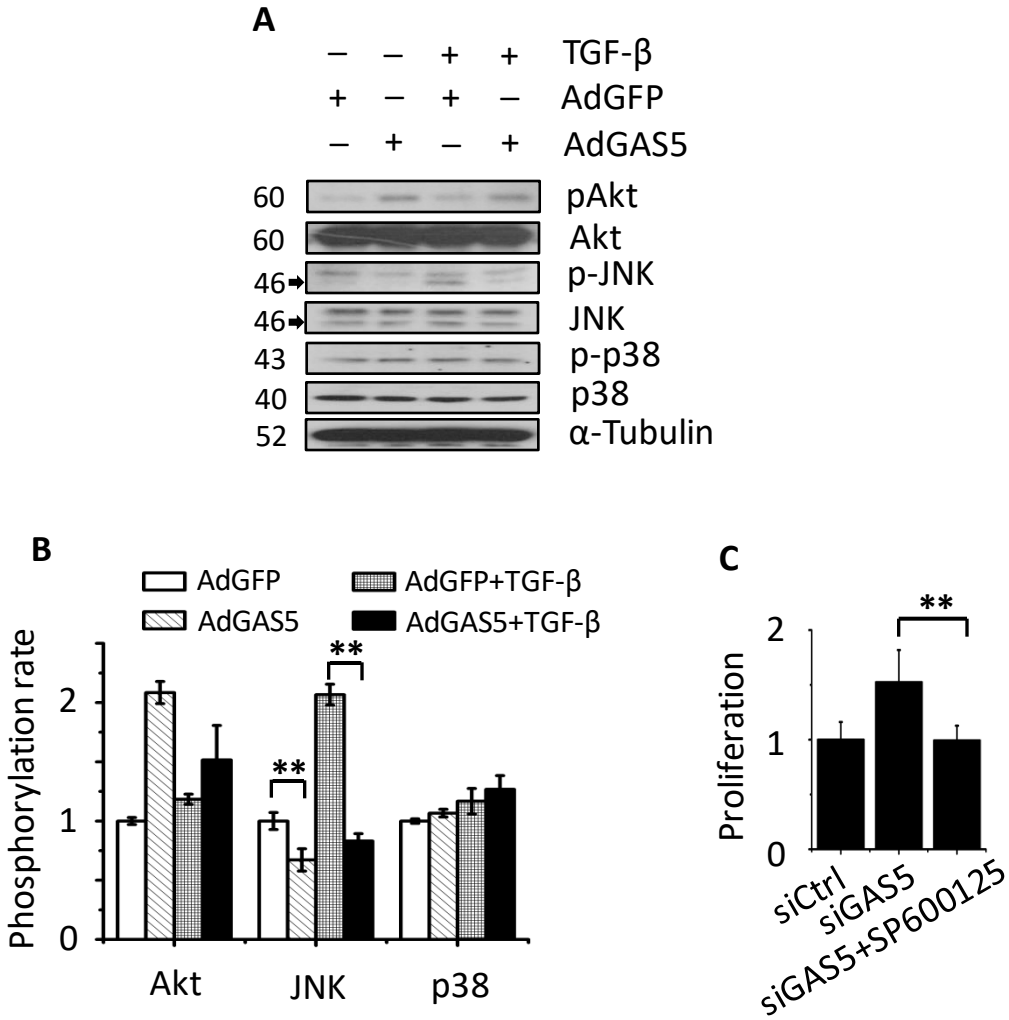

Supplemental Figure S2. GAS5 suppressed TGF-β- induced JNK phosphorylation. **A-B)** 3T3 cells transduced by AdGFP or AdGAS5 were treated with vehicle or 5 ng/ml of TGF-β for 12 hrs. Protein expression or phosphorylation was detected by Western blot (A). Protein phosphorylation in A was normalized to total protein levels (B). **C)** JNK inhibitor SP600125 suppressed siGAS5-enhanced cell proliferation. siCtrl or siGAS5-transfected 3T3 cells were treated with vehicle or 10 μM JNK inhibitor SP600125 for 48 hrs. Cell proliferation was assessed by MTT assay. * $p<0.05$; ** $p<0.01$; n=3.

Supplementary Table 1. Prediction of GAS5 binding to different Smad phosphatases through Incpro (http://bioinfo.bjmu.edu.cn/lncpro/).

Rank	Protein	Value
1	**mmu-Ppm1a**	51.7
2	mmu-Pdp1	41.5
3	mmu-Pp2a	37.7
4	mmu-Mtmr4	37.5
5	mmu-Scp1	34.9
6	mmu-Scp2	27.9